

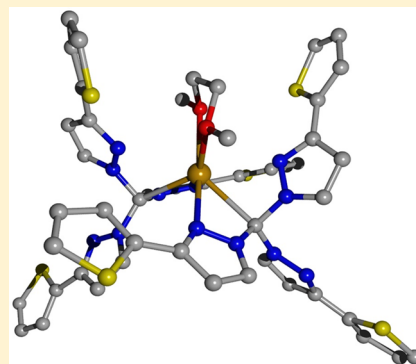
Tris(pyrazolyl)methanides of the Alkaline Earth Metals: Influence of the Substitution Pattern on Stability and Degradation

Christoph Müller, Alexander Koch, Helmar Görls, Sven KriECK, and Matthias Westerhausen*

Institute of Inorganic and Analytical Chemistry (IAAC), Friedrich Schiller University Jena, Humboldtstrasse 8, 07743 Jena, Germany

Supporting Information

ABSTRACT: Trispyrazolylmethanides commonly act as strong tridentate bases toward metal ions. This expected coordination behavior has been observed for tris(3,4,5-trimethylpyrazolyl)methane (**1a**), which yields the alkaline-earth-metal bis[tris(3,4,5-trimethylpyrazolyl)methanides] of magnesium (**1b**), calcium (**1c**), strontium (**1d**), and barium (**1e**) via deprotonation of **1a** with dibutylmagnesium and $[\text{Ae}\{\text{N}(\text{SiMe}_3)_2\}_2]$ (Ae = Mg, Ca, Sr, and Ba, respectively). Barium complex **1e** degrades during recrystallization that was attempted from aromatic hydrocarbons and ethers. In these scorpionate complexes, the metal ions are embedded in distorted octahedral coordination spheres. Contrarily, tris(3-thienylpyrazolyl)methane (**2a**) exhibits a strikingly different reactivity. Dibutylmagnesium is unable to deprotonate **2a**, whereas $[\text{Ae}\{\text{N}(\text{SiMe}_3)_2\}_2]$ (Ae = Ca, Sr, and Ba) smoothly metalates **2a**. However, the primary alkaline-earth-metal bis[tris(3-thienylpyrazolyl)methanides] of Ca (**2c**), Sr (**2d**), and Ba (**2e**) represent intermediates and degrade under the formation of the alkaline-earth-metal bis(3-thienylpyrazolates) of calcium (**3c**), strontium (**3d**), and barium (**3e**) and the elimination of tetrakis(3-thienylpyrazolyl)ethene (**4**). To isolate crystalline compounds, 3-thienylpyrazole has been metalated, and the corresponding derivatives $[(\text{HPz}^{\text{Tp}})_4\text{Mg}(\text{Pz}^{\text{Tp}})_2]$ (**3b**), dinuclear $[(\text{tmeda})\text{Ca}(\text{Pz}^{\text{Tp}})_2]_2$ (**3c**), mononuclear $[(\text{pmdeta})\text{Sr}(\text{Pz}^{\text{Tp}})_2]$ (**3d**), and $[(\text{hmteta})\text{Ba}(\text{Pz}^{\text{Tp}})_2]$ (**3e**) have been structurally characterized. Regardless of the applied stoichiometry, magnesianation of thienylpyrazole **3a** with dibutylmagnesium yields $[(\text{HPz}^{\text{Tp}})_4\text{Mg}(\text{Pz}^{\text{Tp}})_2]$ (**3b**), which is stabilized in the solid state by intramolecular N–H...N...H–N hydrogen bridges. The degradation of $[\text{Ae}\{\text{C}(\text{Pz}^{\text{R}})_3\}_2]$ (R = Ph and Tp) has been studied by quantum chemical methods, the results of which propose an intermediate complex of the nature $\{[(\text{Pz}^{\text{R}})_2\text{C}]_2\text{Ca}\{[\text{Pz}^{\text{R}}]_2\}$; thereafter, the singlet carbenes $[:\text{C}(\text{Pz}^{\text{R}})_2]$ dimerize in the vicinity of the alkaline earth metal to tetrapyrazolyethene, which is liberated from the coordination sphere as a result of it being a very poor ligand for an s-block metal ion.



INTRODUCTION

Tris(pyrazolyl)borates (also called scorpionates) have been studied for many years^{1,2} and represent widely used anionic tridentate ligands in bioinorganic and organometallic chemistry with a rich and diverse coordination behavior.^{3,4} These tridentate anions often stabilize octahedral complexes and act as facial ligands on the basis of steric requirements. The rich and diverse coordination chemistry is aided by the straightforward synthesis and ease of variation of the substitution pattern of the pyrazolyl rings. Substitution of the pyrazolyl bases by softer donor sites, such as imidazol-2-ylidene or thioimidazolyl groups, allows variation of the coordination behavior of these tridentate borates.⁵ Isoelectronic tris(pyrazolyl)methanes and -methanides attracted interest much later than the borate congeners and have been applied mainly to transition-metal-based coordination chemistry and catalysis.⁶ Bis(pyrazolyl)-methanes and -methanides often represent the backbone of heteroscorpionate ligands that contain a different third donor site.⁷ Furthermore, pyrazole-based multidentate ligands allow construction of mononuclear and polynuclear metal complexes.⁸

A closer look at the coordination chemistry of tris(pyrazolyl)borate, -methane, and -methanide toward alkaline earth metal ions reveals that for group II metal ions the borates are a

common ligand system, whereas tris(pyrazolyl)methanides represent a scarce ligand system. Because of the toxicity of beryllium, very few studies illuminate the coordination behavior of this metal. Nevertheless, tris(pyrazolyl)borate anions stabilize (with tetracoordinate metal ions) mononuclear beryllium salts of the type $[\text{HB}(\text{Pz})_3\text{Be-X}]$ (Pz = pyrazolyl; X = Me,⁹ H,^{10,11} F,¹¹ Cl,^{10,11} Br,^{10,11} I,^{10,11} N₃,¹¹ and SH¹⁰).⁹ In contrast, the observation of trinuclear $[\text{HB}(\text{Pz})_3\text{Be-OH}]_3$ has been reported; it has a six-membered Be₃O₃ ring and bidentate tris(pyrazolyl)borate anions.¹² Tris(pyrazolyl)methane and -methanide complexes are known for neither beryllium nor barium, and very few investigations exist with respect to magnesium, calcium, and strontium. Although only tris(pyrazolyl)methane adducts with the $\{[(\text{HC}(\text{Pz})_3)_2\text{Sr}]^{2+}$ fragment have been reported for Sr,¹³ very few reports exist on tris(pyrazolyl)methanides of magnesium^{14–17} and calcium.^{14,18} The tris(pyrazolyl)methane adduct $\{[(\text{HC}(\text{Pz}^{\text{Me}_2})_3)_3\text{Ca}(\text{BF}_4)(\text{thf})_2]^+$ (Pz^{Me₂} = 3,5-dimethylpyrazolyl) has already been tested in the controlled ring-opening polymerization of *rac*-lactide that leads to the formation of an atactic polymer.¹⁹

Received: October 27, 2014

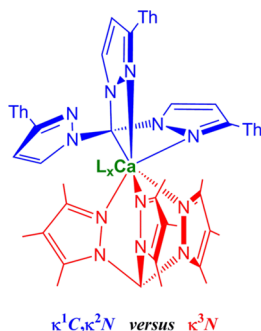
Published: January 7, 2015

Table 1. Coordination Modes of Tris(pyrazolyl)methanes and Tris(pyrazolyl)methanides in Alkaline-Earth-Metal Complexes and Selected Average Bond Lengths^a

compound	mode	Ae	CN(Ae)	Ae–N ^b	Ae–C ^b	ΣNCN ^c	ref
[{HC(Pz ^{Me}) ₃ } ₂ Mg] ²⁺	κ ³ N	Mg	6	216.8		333.9	17
[{HC(Pz ^{Me}) ₃ }MgCl ₂ (thf)]	κ ³ N	Mg	6	227.1		334.6	17
[{HC(Pz ^{Me}) ₃ }Mg{N(SiMe ₃) ₂ } ₂]	κ ² N	Mg	4	214.3		336.1	14
[{Et ₃ Al–C(Pz) ₃ } ₂ Mg]	κ ³ N	Mg	6	214.5		323.0	15
[{C(Pz) ₃ } ₂ Mg]	κ ³ N	Mg	6	214.5		324.2	15
[{C(Pz ^{Me}) ₃ } ₂ Mg]	κ ³ N	Mg	6	219.7		327.3	16
[{C(Pz ^{Me}) ₃ } ₂ Mg]	κ ³ N	Mg	6	218.9		326.7	17
[{C(Pz) ₃ }C{C(Pz ^{Me}) ₃ }Mg]	κ ³ N	Mg	6	217.7		325.7	14
[{C(Pz ^{Me}) ₃ }MgPh(thf)]	κ ³ N	Mg	5	213.6		327.1	17
[{C(Pz ^{Me}) ₃ }Mg{N(SiMe ₃) ₂ } ₂]	κ ³ N	Mg	4	211.5		328.9	14
[{HC(Pz) ₃ } ₂ Ca{CH ₂ (C(O)Me) ₂ } ₂] ²⁺	κ ³ N	Ca	8	255.9		335.7	13
[{HC(Pz ^{Me}) ₃ }Ca(BF ₄)(thf) ₂] ⁺	κ ³ N	Ca	6	251.3		336.2	19
[{C(Pz ^{Me}) ₃ } ₂ Ca]	κ ³ N	Ca	6	244.8		331.7	14
[{C(Pz ^{Me}) ₃ }Ca{N(SiMe ₃) ₂ }(thf)]	κ ³ N	Ca	5	243.4		333.4	14
[{C(Pz ^{Ph}) ₃ } ₂ Ca(dme)]	κ ¹ C,κ ² N	Ca	8	262.6	260.4	329.5	18
[{HC(Pz) ₃ } ₂ Sr{CH ₂ (C(O)Me) ₂ } ₂] ²⁺	κ ³ N	Sr	8	268.4		334.8	13
[{HC(Pz) ₃ } ₂ Sr(O=CMe) ₂] ²⁺	κ ³ N	Sr	8	267.9		336.9	13
[{HC(Pz) ₃ } ₂ Sr(BF ₄) ₂]	κ ³ N	Sr	8	272.7		335.3	13

^aAe = alkaline earth metal, dme = 1,2-dimethoxyethane, Py = pyrazolyl, Pz^{Me} = 3,5-dimethylpyrazolyl, Pz^{Ph} = 3-phenylpyrazolyl, thf = tetrahydrofuran, CN(Ae) = coordination number of the alkaline earth metal ion. ^bBond lengths given in picometers. ^cΣNCN angle sum of C considering only NCN bond angles, represented in degrees.

Tris(pyrazolyl)methanes and -methanides commonly act as tridentate bases via their nitrogen bases (Table 1) and have coordination numbers between four and eight, depending on the substitution pattern of the pyrazolyl substituents, the bulkiness of the coligands, and the size of the alkaline earth metal ions. There are only two exceptions: (1) In [{HC-(Pz^{Me})₃}Mg{N(SiMe₃)₂}₂], the bulky bis(trimethylsilyl)amido anions push one pyrazolyl side arm to the periphery of the complex, changing tris(pyrazolyl)methane to a bidentate ligand.¹⁴ (2) The κ¹C,κ²N coordination mode of the tris(3-phenylpyrazolyl)methanide anion in [{C(Pz^{Ph})₃}₂Ca(dme)] is unique in alkaline-earth-metal-based coordination chemistry (Scheme 1);¹⁸ however, a similar coordination behavior has

Scheme 1. Representation of the κ³N- and κ¹C,κ²N-Coordination Modes (Red and Blue, Respectively) of Tris(pyrazolyl)methanides at a Calcium Ion^a

^aAlkyl substituents stabilize the κ³N-binding fashion, whereas aromatic groups such as phenyl or thienyl (Th) support the κ¹C,κ²N-binding mode.

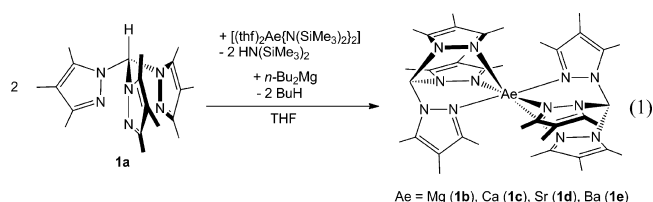
already been described for the unsubstituted tris(pyrazolyl)-methanide anion in the cadmium complex [{κ³N-C(Pz^{Me})₃}₂]-{κ¹C,κ²N-C(Pz)₃}Cd].¹⁴ On the basis of taking only NCN bond angles into account, the angle sum of the tris(pyrazolyl)-substituted

carbon atom of the magnesium-bound methane ligands has an angle sum greater than 330°, whereas the deprotonation and formation of the magnesium-bound methanide leads to angle sums less than 330°. Such a clear differentiation is not observed for the calcium derivatives, whereas no strontium-centered methanide complexes are available for comparison. The Ae–N bond lengths depend mainly on the steric strain that is induced by large coordination numbers and on substituents in the vicinity of the metal ions.

Unexpectedly, [{κ¹C,κ²N-C(Pz^{Ph})₃}₂Ca(dme)] proved to be significantly less stable than all other known tris(pyrazolyl)-methanide congeners. Degradation of this complex yields dinuclear calcium bis(3-phenylpyrazolate), which was stabilized and crystallized as a tmeda adduct.¹⁸ To expand the knowledge of the structures and stability of tris(pyrazolyl)methanide complexes of magnesium and the heavier alkaline earth metals, we prepared their tris(3,4,5-trimethylpyrazolyl)methanide ([C(Pz^{Me})₃]) and tris(thiophen-2-ylpyrazolyl)methanide ([C(Pz^{TP})₃]) derivatives.

RESULTS AND DISCUSSION

Tris(3,4,5-trimethylpyrazolyl)methanides. Tris(3,4,5-trimethylpyrazolyl)methane (1a)²⁰ contains an acidic proton and can easily be metalated with commercially available dibutylmagnesium and [(thf)₂Ae{N(SiMe₃)₂}₂] (Ae = Ca, Sr, and Ba)^{21,22} in tetrahydrofuran, as shown in eq 1. After the



removal of all of the volatiles, the residues were extracted with toluene. Cooling of these solutions led to the formation of colorless crystals of [κ³N-C(Pz^{Me})₃}₂Ae] (Ae = Mg (1b),

Ca (**1c**), Sr (**1d**), and Ba (**1e**). All of these complexes precipitated without coordinated solvent molecules.

The ^1H NMR parameters of the alkaline-earth-metal-containing bis[$\kappa^3\text{N}$ -tris(3,4,5-trimethylpyrazolyl)methanides] are very similar and lack significant dependency on size or nature of the metal atom, suggesting very similar coordination behavior among these divalent ions. However, the strontium derivative (**1d**) is only sparingly soluble in common organic solvents, so no reliable ^{13}C NMR shifts were obtained. The barium complex (**1e**) shows different behavior and is soluble in toluene, allowing the elucidation of NMR values. In the ESI mass spectrum, the molecular ion peak was detected. However, recrystallization efforts led to the decomposition of this complex, and numerous resonances were observed in the NMR spectra. Therefore, we were able to determine only the crystal structures of the complexes of magnesium, calcium, and strontium.

For comparison, the molecular structure of tris(3,4,5-trimethylpyrazolyl)methane (**1a**), which precipitated as a clathrate with tmeda from 1,2-bis(dimethylamino)ethane, is depicted in Figure 1; in this representation, cocrystallized

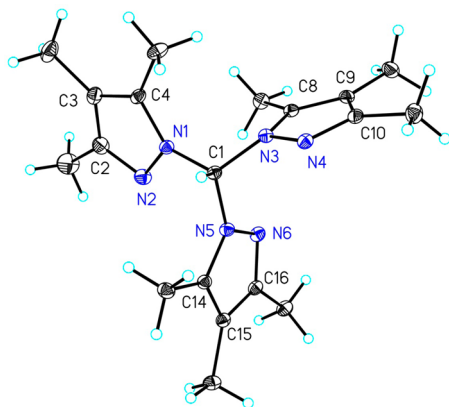


Figure 1. Molecular structure and numbering scheme of compound **1a**. The ellipsoids represent a probability of 30%; H atoms are drawn with arbitrary radii. Cocrystallized tmeda is not shown.

tmeda is neglected for clarity. In **1a**, the N–C1–N bond angles are larger than the tetrahedral angle, resulting in a $\Sigma\text{N–C1–N}$ angle sum of 334.0° . Because of the methyl group at the fifth position of each of the pyrazolyl rings, the C1–N–C angles are large, leading to significantly different distal C1–N–C and proximal C1–N–N bond angles.

The molecular structure and numbering scheme of magnesium bis[$\kappa^3\text{N}$ -tris(3,4,5-trimethylpyrazolyl)methanide] (**1b**) are shown in Figure S1. The magnesium atom lies on an inversion center and exhibits a slightly distorted octahedral environment with intraligand N–Mg1–N angles of $83.97(6)^\circ$ and larger cisoid interligand N–Mg1–N bond angles of $96.03(6)^\circ$. The Mg1–N2 bond length (218.5(2) pm) lies in the range characteristic of other tris(pyrazolyl)methanides of magnesium (see Table 2). In agreement with earlier studies, the $\Sigma\text{N–C1–N}$ angle sum (327.2°) is less than that of the corresponding methane compound (**1a**). Because of the coordination to magnesium, the C1–N1–C2 and C1–N1–N2 bond angles are rather similar.

The molecular structure and numbering scheme of calcium bis[$\kappa^3\text{N}$ -tris(3,4,5-trimethylpyrazolyl)methanide] (**1c**) are depicted in Figure S2. Again, the alkaline earth metal atom is

embedded in a distorted octahedral environment with an average Ca1–N distance of 244.1 pm.

The strontium derivative (**1d**) exhibits a very similar molecular structure (Figure 2). Because of the larger atomic radius

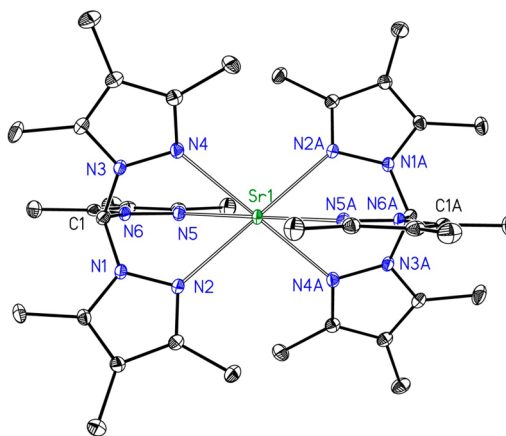


Figure 2. Molecular structure and numbering scheme of compound **1d**. Symmetry-related atoms ($-x+1, -y, -z$) are marked with the letter A. The ellipsoids represent a probability of 30%; H atoms are omitted for the sake of clarity.

of this alkaline earth metal and a very similar bite angle of the ligand, the intraligand and cisoid interligand N–Sr1–N bond angles (average values = 73.9 and 106.1° , respectively) differ by more than 30° . The larger metal atom pushes the pyrazolyl bases apart; hence, a greater $\Sigma\text{N–C1–N}$ angle sum (334.0°) is observed. In comparison to the tris(3,5-dimethylpyrazolyl)methane adducts of octacoordinated strontium (with an average Sr–N distance of 269.7 pm),¹³ significantly smaller Sr–N bond lengths are observed for **1d** (which has a hexacoordinated metal atom). These smaller Sr–N values are a consequence of the decreased coordination number of the metal center and also of the additional electrostatic attraction in complex **1d**.

Table 2 summarizes the average values of selected structural parameters. The Ae–N bond lengths reflect the increasing radius of the alkaline earth metals from **1b** to **1d**. Because of the fact that the tris(3,4,5-trimethylpyrazolyl)methanide anions are rather inflexible, the increasing size of the atomic radii of the metals leads to more acute intraligand N–Ae–N bond angles. The bond lengths of the tris(3,4,5-trimethylpyrazolyl)methanide anions are very similar for all complexes and show negligible deviations from parameters of tris(3,4,5-trimethylpyrazolyl)methane (**1a**). The $\Sigma\text{N–C1–N}$ angle sums at C1 are all greater than 330° , with the exception of that of the magnesium derivative. One would expect smaller angle sums for methanides than for the neutral methane (**1a**); however, larger metal ions push the pyrazolyl bases apart and increase the angle sums at C1.

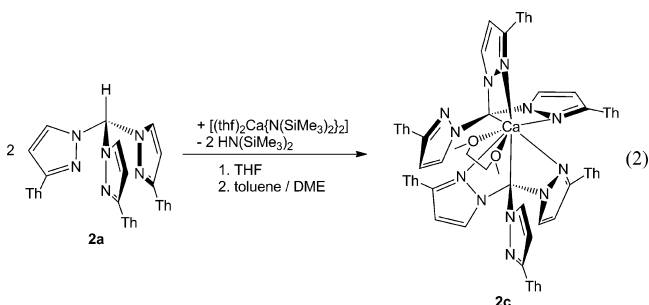
Tris(3-thiophen-2-ylpyrazolyl)methanides. In contrast to unsubstituted and methyl-substituted tris(pyrazolyl)methanides, the phenyl-substituted pyrazolyl groups destabilize the methanide anion.¹⁸ On the basis of this observation, we investigated the metalation of tris(3-thiophen-2-ylpyrazolyl)methane ($\text{HC}\{\text{Pz}^{\text{Tp}}\}_3$, **2a**) with $[(\text{thf})_2\text{Ae}\{\text{N}(\text{SiMe}_3)_2\}_2]$.^{21,22} Surprisingly, the magnesium derivative is too inert, and deprotonation of **2a** did not succeed. The reaction of $[(\text{thf})_2\text{Ca}\{\text{N}(\text{SiMe}_3)_2\}_2]$ with **2a** in tetrahydrofuran at -40°C and subsequent recrystallization from a solvent mixture of

Table 2. Comparison of Selected Structural Parameters of Tris(3,4,5-trimethylpyrazolyl)methane (1a) and Tris(thiophen-2-ylpyrazolyl)methane (2a) as Well as Their Alkaline-Earth-Metal Derivatives^a

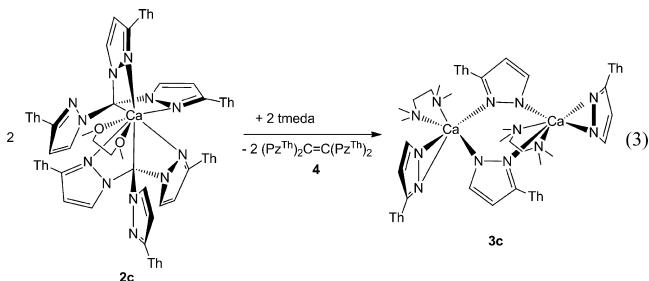
	1a	1b	1c	1d	2a	2c
Ae	H	Mg	Ca	Sr	H	Ca
mode	$\kappa^1\text{C}$	$\kappa^3\text{N}$	$\kappa^3\text{N}$	$\kappa^3\text{N}$	$\kappa^1\text{C}$	$\kappa^1\text{C}, \kappa^2\text{N}$
Ae–C1	100				97(2)	258.0(3)
Ae–N2		218.5(2)	244.3(2)	258.3(2)		258.4(2)
Ae–N4			244.3(2)	258.6(2)		
Ae–N6			244.1(2)	258.4(2)		282.8(3)
C1–N1	146.6(2)	144.5(2)	143.8(3)	144.6(3)	145.0(3)	145.8(4)
C1–N3	144.7(2)		144.6(3)	144.0(3)	144.5(3)	144.6(4)
C1–N5	143.7(2)		144.6(3)	145.2(3)	144.2(3)	145.2(4)
N1–N2	136.4(2)	137.8(2)	138.3(3)	137.9(3)	136.2(2)	137.1(3)
N3–N4	137.4(2)		137.9(3)	138.0(3)	136.6(2)	137.3(3)
N5–N6	136.9(2)		138.1(3)	137.7(3)	137.0(2)	136.5(3)
N1–C2	136.5(2)	135.5(3)	136.1(3)	135.8(3)	135.9(3)	135.5(4)
C2–C3	138.1(2)	138.1(3)	137.6(4)	138.3(3)	136.3(3)	136.6(5)
C3–C4	140.9(2)	140.7(3)	140.7(4)	140.2(3)	141.4(3)	140.7(4)
N2–C4	133.2(2)	133.3(3)	133.4(3)	133.8(3)	133.9(3)	134.4(4)
N2–Ae–N4		83.97(6)	78.30(7)	73.85(6)		
N2–Ae–N6			77.79(7)	74.43(6)		94.13(8)
N4–Ae–N6			77.31(7)	73.28(6)		
N1–C1–N3	111.59(11)	109.07(14)	111.0(2)	111.96(19)	109.49(16)	110.2(2)
N1–C1–N5	110.91(11)		111.2(2)	111.00(18)	110.47(16)	110.1(2)
N3–C1–N5	111.51(11)		110.6(2)	111.05(19)	112.01(17)	110.8(2)
$\Sigma\text{N–C1–N}^b$	334.01	327.21	332.8	334.01	331.97	331.1

^aAe = hydrogen or alkaline earth metal. Bond angles given in degrees. ^b ΣNCN angle sum of C considers only N–C–N bond angles.

toluene and 1,2-dimethoxyethane yielded $[\{\kappa^1\text{C}, \kappa^2\text{N–C–(Pz}^{\text{TP}})_3\}_2\text{Ca}(\text{dme})]$ (2c), as shown in eq 2. Because of decomposition during isolation and handling, reliable combustion analyses were unavailable.



Addition of tmeda to a solution of 2c or recrystallization of the initial product from a solvent mixture of toluene and tmeda yielded dinuclear $[(\text{tmeda})\text{Ca}(\text{Pz}^{\text{TP}})_2]_2$ (3c) as shown in eq 3. The more reactive bis(trimethylsilyl)amides of strontium and barium immediately gave the 3-thienylpyrazolates. The formation



of intermediate tris(3-thienylpyrazolyl)methanide complexes can be assumed; however, we were unable to isolate such species.

To study the scope of this degradation reaction, $\text{HC}\{\text{Pz}^{\text{TP}}\}_3$ (2a) was reacted with $\text{LiN}(\text{SiMe}_3)_2$, $[(\text{thf})_2\text{Ca}\{\text{N}(\text{SiMe}_3)_2\}_2]$, $[(\text{dme})_2\text{Sr}\{\text{N}(\text{SiMe}_3)_2\}_2]$, and $[(\text{dme})_2\text{Ba}\{\text{N}(\text{SiMe}_3)_2\}_2]$ in tetrahydrofuran or 1,2-dimethoxyethane. Thereafter, hydrolysis and extraction with chloroform gave a mixture of $\text{HC}\{\text{Pz}^{\text{TP}}\}_3$ (2a), tetrakis(3-thienylpyrazolyl)ethene (4), and HPz^{TP} (3a). This finding shows that the sp^2 -hybridized carbon atoms in position 3, as part of the π systems, significantly destabilize the tris(pyrazolyl)methanide backbone. On the basis of this observation, quantum chemical calculations on the degradation of this ligand were subsequently carried out.

The molecular structure and numbering scheme of $\text{HC}\{\text{Pz}^{\text{TP}}\}_3$ (2a) are depicted in Figure 3. The central tertiary carbon atom exhibits a slightly widened ΣNCN angle sum

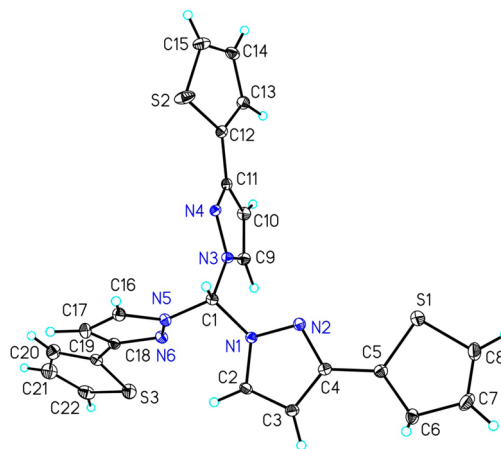


Figure 3. Molecular structure and numbering scheme of ligand 2a. The ellipsoids represent a probability of 30%; H atoms are shown with arbitrary radii.

(Table 2), with characteristic C1–N single bonds. Within the pyrazolyl moieties, a partial charge delocalization is observed (comparable N1–C2 and N2–C4 bond lengths = 135.9(3) and 133.9(3) pm, respectively); however, the C2–C3 and C3–C4 bond lengths of 136.3(3) and 141.4(3) pm, respectively, are significantly different. The C4–C5 distance (between the pyrazolyl and thienyl rings) of 145.9(3) pm is characteristic of a single bond between sp^2 -hybridized carbon atoms. Because of the repulsive forces between the ortho hydrogen atoms of the pyrazolyl rings, significantly different C1–N1–N2 and C1–N1–C2 bond angles are observed (118.0(2) and 128.3(2)°, respectively). Comparable structural parameters were also found for the other 3-thienylpyrazolyl units.

The calcium atom in complex **2c** shows an unusually large coordination number of eight (to two tridentate scorpionate anions and one bidentate dme ligand). The molecular structure and numbering scheme for **2c** are depicted in Figure 4.

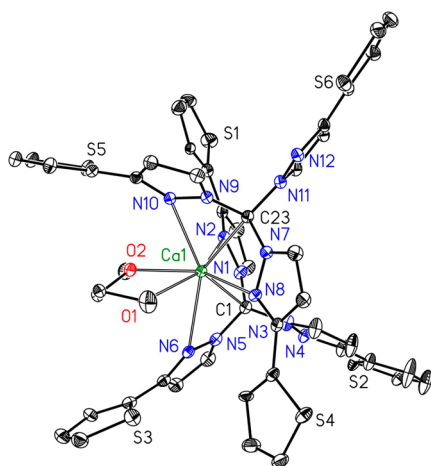


Figure 4. Molecular structure and numbering scheme of compound **2c**. The ellipsoids represent a probability of 30%; H atoms are omitted for the sake of clarity.

The tris(3-thiophen-2-ylpyrazolyl)methanide anions exhibit a unique κ^1C, κ^2N coordination mode and bind via two pyrazolyl bases and the methanide site with one free side arm. The calcium–carbon bond lengths of 258.0(3) and 259.9(3) pm lie in a range characteristic of alkylcalcium²³ and arylcalcium derivatives.²⁴ The ligated bis(pyrazolyl)methanide bases show an asymmetric coordination mode with short Ca1–N bonds (Ca1–N2 = 258.4(2) pm and Ca1–N8 = 257.9(2) pm) and long Ca1–N bonds (Ca1–N6 = 282.8(3) pm and Ca1–N10 = 269.6(2) pm). Nevertheless, this binding mode does not distort the tris(pyrazolyl)methanide fragment, and very similar N–C1–N bond angles are found. The Ca1–O1 and Ca1–O2 bond lengths to the bidentate ether exhibit characteristic values (average value = 244.9 pm). Therefore, the coordination number of Ca1 can best be described as 6 + 2.

The X-ray structure determination of tetrakis(3-thienylpyrazolyl)ethene (**4**) was hampered by a two-site disordering of the thienyl groups. Figure 5 shows the molecular structure of **4** with only one orientation of the disordered thienyl substituents. The C1=C1A bond length of this C_2 -symmetric molecule has a characteristic double bond value of 133(1) pm.

Quantum Chemical Studies. To clarify the strikingly different behaviors of the tris(3,4,5-trimethylpyrazolyl)methanides (**1**) and tris(3-thienylpyrazolyl)methanides (**2**), we carried out quantum chemical studies. In a simplified picture,

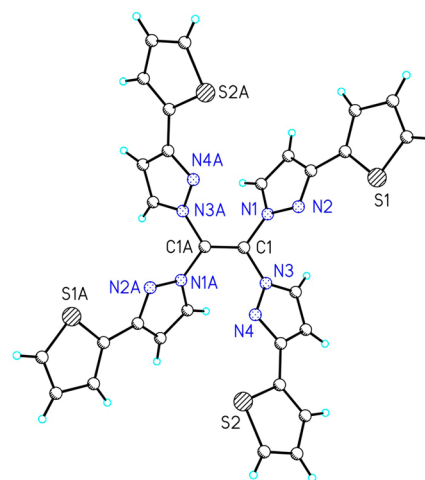
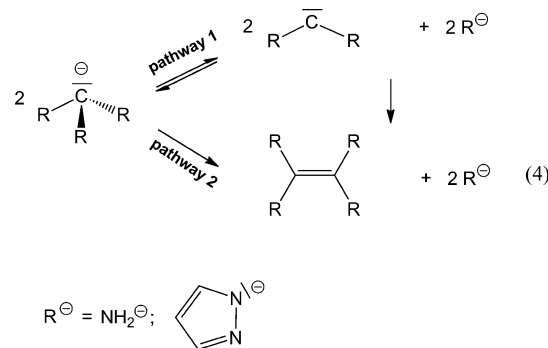


Figure 5. Structural motif and numbering scheme of compound **4**. Symmetry-related atoms ($-x, -y, -z+0.5$) are marked with the letter A. All atoms are drawn with arbitrary radii. The two-site disordering of the thienyl groups is omitted for the sake of clarity.

tris(pyrazolyl)methanides may be considered as a Lewis acid–base adduct, with the Lewis base being a pyrazolate and the Lewis acid being a bis(pyrazolyl)carbene. Theoretical investigations showed that the singlet of diaminocarbene ($[(H_2N)_2C]$) is significantly lower in energy than the triplet state, differing by 52.0–57.1 kcal mol⁻¹ (depending on the basis sets).^{25,26} Therefore, the tris(pyrazolyl)methanide anions of **2** could dissociate into a pyrazolate anion and a bis(pyrazolyl)carbene; dimerization of the carbene leads to tetrakis(pyrazolyl)ethene, thus removing this species from the equilibrium. To support this mechanism, we carried out quantum chemical studies of the degradation of tris(amino)methanide ($[(H_2N)_3C^-]$) and tris(pyrazolyl)methanide ($[(Pz)_3C^-]$, eq 4). The fact that the



singlet state of these carbenes is stabilized by a charge transfer from the lone electron pair at N into the empty p orbital at the carbon atom causes the dissociation of these methanides. A simple dissociation of $[CR_3^-]$ into the singlet carbene ($[:CR_2]$ and $[R^-]$, R = NH₂ and Pz) is disadvantageous (Table 3, pathway 1), but the formation of ethene ($[R_2C=CR_2]$) leads to a favored reaction (Table 3, pathway 2).

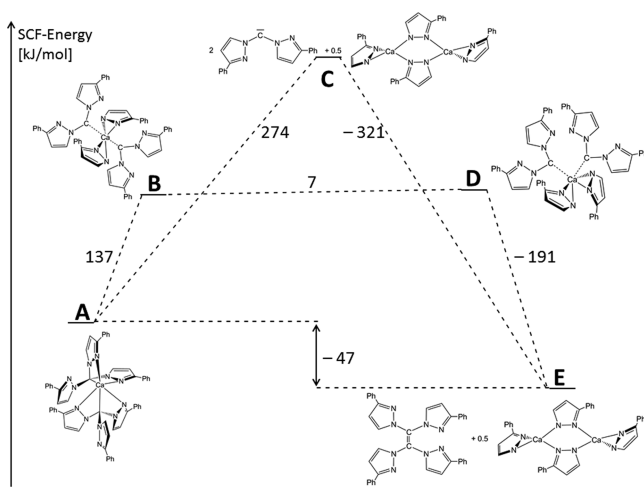
Why do tris(3-thienylpyrazolyl)methanides (**2**) and tris(3-phenylpyrazolyl)methanides¹⁸ degrade so easily whereas tris(3,4,5-trimethylpyrazolyl)methanides (**1**) and tris(3,5-dimethylpyrazolyl)methanides^{14,18} are stable at ambient conditions? We propose that the unique κ^1C, κ^2N coordination mode might be responsible for the preferential degradation process (Scheme 2). Therefore, we calculated two reaction pathways; both take into account the splitting of $[C(Pz^{\text{Ph}})_3^-]$ into a singlet

Table 3. Calculated Enthalpies of the Above Reactions at the B3LYP/aug-cc-pVTZ or MP2/aug-cc-pVTZ Level of Theory^a

substituent R	method	pathway 1 ^b	pathway 2 ^b
amide	B3LYP	72 (27)	-23 (-61)
	MP2	98 (53)	-40 (-77)
pyrazolate	B3LYP	133 (84)	-46 (-93)

^aRepresented in kilojoules per mole. ^bGibbs free energies are given in parentheses and are represented in kilojoules per mole.

Scheme 2. Computed Pathways for the Decomposition of [$\kappa^1\text{C},\kappa^2\text{N-C}(\text{Pz}^{\text{Ph}})_3\text{Ca}$] with the B3LYP/6-++31G** Level of Theory

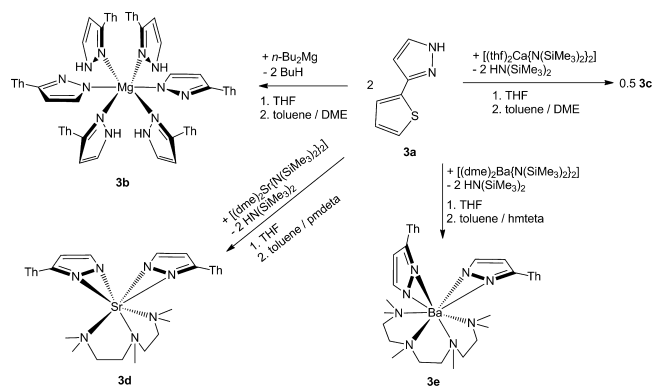


carbene ($[:\text{C}(\text{Pz}^{\text{Ph}})_2]$) and anion ($\text{Pz}^{\text{Ph}-}$). The disadvantageous pathway includes a dissociation step and the formation of free carbene; in the favored pathway, however, the carbenes remain in the coordination sphere of the calcium atom, yielding $[(\text{Pz}^{\text{Ph}})_2\text{C}]_2\text{Ca}[\text{Pz}^{\text{Ph}}_2]$. The rearrangement processes are nearly electroneutral, allowing close contact between both carbene species and the formation of alkene $[(\text{Pz}^{\text{Ph}})_2\text{C}=\text{C}(\text{Pz}^{\text{Ph}})_2]$, which is liberated thereafter and leads to the formation of a dimeric calcium bis(pyrazolate).

Because tris(3-phenylpyrazolyl)methanide and tris(3-thienylpyrazolyl)methanide bind via the carbon atoms and the pyrazolyl bases, the formed carbenes are already very close to each other. It has been previously shown that carbenes are suitable ligands for calcium ions;²⁷ therefore, these ligated carbenes remain close to each other, favoring dimerization. In contrast, alkenes are very poor ligands in alkaline-earth-metal-based coordination chemistry; they are released and replaced by stronger Lewis bases, such as ethers, amines, or, via dimerization, additional pyrazolate bases. In alkyl-substituted tris(pyrazolyl)methanides, the carbon atoms are turned to the outside of the complexes, hampering an intramolecular formation and the recombination of the carbenes as well as an intermolecular reaction due to the steric protection by the methyl groups at the fifth position of each of the pyrazolyl substituents. Additionally, the mesomeric influence of aryl and (aromatic) thienyl groups enhances the charge on the pyrazolyl rings and supports the degradation as a consequence of the increased electrostatic repulsion among the negative methanide moiety and the electron-enriched pyrazolyl groups.

3-Thiophen-2-ylpyrazolates. The coordination behavior of pyrazolates has been studied for many years.^{8,22,28} To verify

the degradation products from the metalation of $\text{HC}\{\text{Pz}^{\text{TP}}\}_3$ (**2a**) with $[(\text{L})_2\text{Ae}\{\text{N}(\text{SiMe}_3)_2\}_2]$, we reacted these alkaline-earth-metal-containing bis[bis(trimethylsilyl)amides] with 2 equiv of 3-thiophen-2-ylpyrazole (**3a**) in tetrahydrofuran. For the preparation of the magnesium derivative, deprotonation of HPz^{TP} was carried out with commercially available dibutylmagnesium, yielding $[(\text{HPz}^{\text{TP}})_4\text{Mg}(\text{Pz}^{\text{TP}})_2]$ (**3b**) regardless of the applied stoichiometry. To isolate the crystalline form of the compounds, amino bases were added (eq 5). The



dentificity of the amino bases was adapted to the size of the alkaline earth metal ion. Thus, we were able to isolate and structurally investigate $[(\text{HPz}^{\text{TP}})_4\text{Mg}(\text{Pz}^{\text{TP}})_2]$ (**3b**), dinuclear $[(\text{tmeda})\text{Ca}(\text{Pz}^{\text{TP}})_2]_2$ (**3c**) (which is identical to the derivative prepared via degradation of **2c**), mononuclear $[(\text{pmdeta})\text{Sr}(\text{Pz}^{\text{TP}})_2]$ (**3d**), and $[(\text{hmteta})\text{Ba}(\text{Pz}^{\text{TP}})_2]$ (**3e**).

The molecular structure of $[(\text{HPz}^{\text{Th}})_4\text{Mg}(\text{Pz}^{\text{Th}})_2]$ (**3b**) is depicted in Figure 6. The N-bound hydrogen atoms were

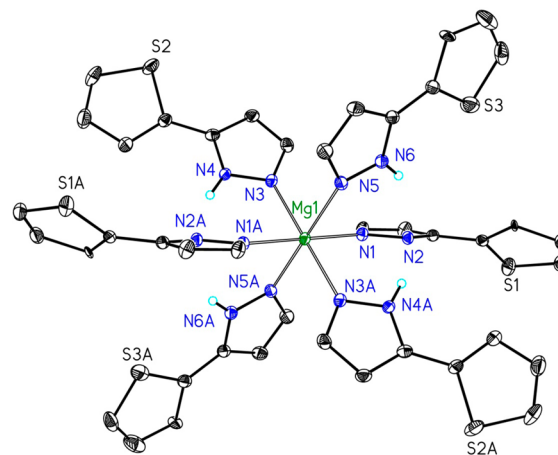


Figure 6. Molecular structure and numbering scheme of compound **3b**. Symmetry-related atoms ($-x+2, -y+1, -z+1$) are marked with the letter A. The ellipsoids represent a probability of 30%; H atoms are omitted for the sake of clarity, with the exception of the N-bound H atoms in order to clarify the stabilizing $\text{N}-\text{H}\cdots\text{N}\cdots\text{H}-\text{N}$ hydrogen bridges.

refined isotropically; therefore, they are included in the representation. Because of the crystallographic inversion symmetry, the pyrazolate anions are strictly trans arranged. Because of the stronger electrostatic attraction, the $\text{Mg1}-\text{N1}$ bond length (216.3(3) pm) is about 5 pm smaller than the distances between Mg1 and neutral pyrazole bases. The N-H moieties are directed to the pyrazolate N2 atom, forming weak hydrogen bridges of the type $\text{N}-\text{H}\cdots\text{N}\cdots\text{H}-\text{N}$. These hydrogen bridges

also stabilize this octahedral complex and offer an explanation for the finding that this complex is formed regardless of the applied stoichiometry and the fact that the pyrazolate anions exhibit an η^1 coordination mode.

The molecular structure and numbering scheme of dinuclear $[(\text{tmeda})\text{Ca}(\text{Pz}^{\text{Th}})_2]_2$ (**3c**) are depicted in Figure 7. The middle

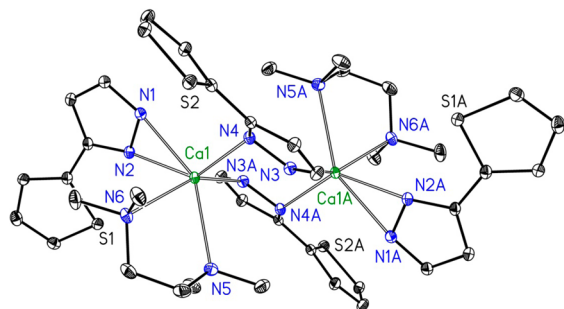


Figure 7. Molecular structure and numbering scheme of compound **3c**. Symmetry-related atoms ($-x+1, -y+1, -z+2$) are marked with the letter A. The ellipsoids represent a probability of 30%; H atoms are omitted for the sake of clarity.

centrosymmetric Ca_2N_4 ring exhibits a chair conformation with Ca1-N4 and Ca1-N3A bond lengths of 240.7(2) and 247.5(2) pm, respectively. The pyrazolate anions show terminal and bridging coordination modes of $\eta^2\text{-Pz}^{\text{Th}}$ and $\mu\text{-}\eta^1\text{:}\eta\text{-Pz}^{\text{Th}}$, respectively. The terminally bound pyrazolate shows a symmetric coordination with bond lengths of 239.3(3) and 239.4(2) pm. Because of the lack of anionic charge, the Ca1-N5 and Ca1-N6 distances to the tmeda ligand (257.8(3) and 257.4(29) pm, respectively) are significantly enhanced.

The molecular structure and numbering scheme of mononuclear $[(\text{pmdeta})\text{Sr}(\text{Pz}^{\text{Th}})_2]$ (**3d**) are represented in Figure 8.

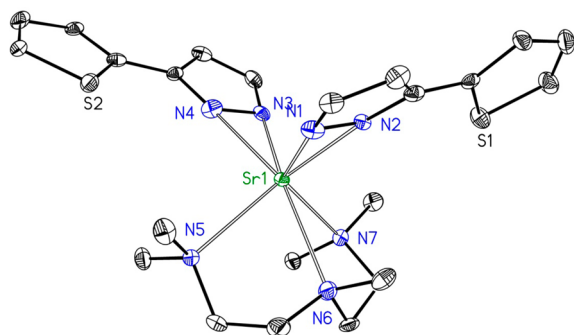


Figure 8. Molecular structure and numbering scheme of compound **3d**. The ellipsoids represent a probability of 30%; H atoms are omitted for the sake of clarity.

The pyrazolate anions bind in an η^2 -manner with Sr1-N bond lengths between 251.1(5) and 255.8(7) pm.

The molecular structure and numbering scheme of $[(\text{hmteta})\text{Ba}(\text{Pz}^{\text{Th}})_2]$ (**3e**) are displayed in Figure 9. The asymmetric unit contains two molecules, **A** and **B**, but only **A** is shown. The cis-arranged pyrazolate anions exhibit an η^2 coordination mode with $\text{Ba1A-N}_{\text{Pz}}$ bond lengths between 271.9(5) and 286.5(5) pm, whereas those bond lengths to the tetradentate hmteta ligand are elongated to values between 285.0(4) and 302.7(4) pm.

In all of these pyrazolates, the alkaline earth metals bind to the nitrogen atoms. Despite the fact that pyrazolate anions

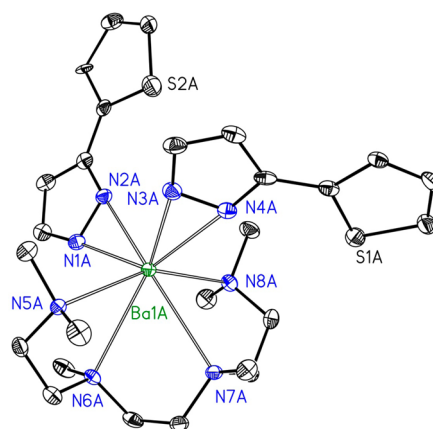


Figure 9. Molecular structure and numbering scheme of compound **3e**. This compound crystallizes as two crystallographically independent molecules (**A** and **B**); only **A** is depicted. The ellipsoids represent a probability of 30%; H atoms are omitted for the sake of clarity.

exhibit a highly aromatic character, no side-on coordination to the π system was observed. Terminally bound pyrazolates prefer η^2 coordination modes unless other factors such as a hydrogen bridge framework, as observed in the magnesium derivative **3b**, stabilize the deviating binding modes.

CONCLUSIONS

In agreement with earlier investigations, tris(3,4,5-trimethylpyrazolyl)methane (**1a**) can easily be deprotonated with dibutylmagnesium and the bis(trimethylsilyl)amides of the alkaline earth metals, yielding the corresponding bis[tris(3,4,5-trimethylpyrazolyl)methanides] of magnesium (**1b**), calcium (**1c**), strontium (**1d**), and barium (**1e**). In all of these complexes, the tris(pyrazolyl)methanide anion exhibits the expected $\kappa^3\text{N}$ coordination mode, leading to distorted octahedral environments of magnesium, calcium, and strontium in the solid state. The barium complex decomposed during recrystallization experiments.

In contrast to this finding, tris(3-phenylpyrazolyl)methane and tris(3-thienylpyrazolyl)methane (**2a**) show strikingly different reactivities. Although magnesianation of tris(3-thienylpyrazolyl)methane (**2a**) did not succeed with dibutylmagnesium and magnesium bis[bis(trimethylsilyl)amide] in tetrahydrofuran, metalation with the bis(trimethylsilyl)amides of the heavier homologous alkaline earth metals proceeded smoothly. In the crystalline state, the methanide anion in the calcium derivative $[(\text{dme})\text{Ca}\{\text{C}(\text{Pz}^{\text{Th}})_3\}_2]$, **2c** showed a unique $\kappa^1\text{C}, \kappa^2\text{N}$ coordination behavior with rather short Ca-C bond lengths. This complex is rather labile, and it degrades into tetrakis(3-thiophen-2-ylpyrazol-1-yl)ethene (**4**) and calcium bis(3-thienylpyrazolate), which was crystallized as the tmeda adduct. To verify this, the alkaline earth metal bis(3-thienylpyrazolates) of magnesium (**3b**), calcium (**3c**), strontium (**3d**), and barium (**3e**) were prepared via deprotonation of the 3-thienylpyrazole (**3a**). Because of the immediate degradation of the initial metalation product, the reaction of $[(\text{dme})_2\text{Ae}\{\text{N}(\text{SiMe}_3)_2\}_2]$ with $\text{HC}(\text{Pz}^{\text{Th}})_3$ yielded the corresponding ethene derivative (**4**) and the 3-thienylpyrazolates (**3d,e**).

Deprotonation of tris(pyrazolyl)methanes leads to decreased ΣNCN angle sums because the covalent C-H bond is less demanding than a free electron pair containing the negative charge. Electrostatic repulsion between the anionic charge of the methanide anion and the electron-rich nitrogen atoms of

the pyrazolyl groups enhances the intraligand strain. Large metal atoms push the pyrazolyl rings apart and increase the Σ NCN angle sum, thus increasing the steric pressure. The tris(pyrazolyl)methanide complexes are stable if the negatively charged methanide functionalities show a large spatial separation, as observed in $[\text{Ae}\{\kappa^3\text{N-C}(\text{Pz}^{\text{Me}_3})_3\}_2]$.

As discussed above, the enlargement of the Σ NCN angle sum leads to enhanced intramolecular strain and repulsion between the electron pair and neighboring C1–N bonds. To reduce this electrostatic repulsion, a $\kappa^1\text{C},\kappa^2\text{N}$ coordination mode with Ca–C bonds is realized in $[(\text{dme})\text{Ca}\{\text{C}(\text{Pz}^{\text{Tp}})_3\}_2]$ (**2c**), which leads to two carbanions that are close to each other. Transfer of the negative charge to one pyrazolyl unit reduces the strain, but this charge transfer also initiates intermediate formation of a coordinated carbene-like species that could attack the other $\kappa^1\text{C},\kappa^2\text{N}$ -bound ligand in the vicinity of the calcium ion. This fast reaction immediately yields tetrakis(pyrazolyl)ethene without any other detectable intermediates. On the basis of our findings, it may be assumed that this charge-transfer step requires a bulky group with an +M effect (such as phenyl and thienyl) in order to change the coordination from a $\kappa^3\text{N}$ mode to a $\kappa^1\text{C},\kappa^2\text{N}$ mode. The +M effect leads to enhancement of the charge on the pyrazolyl ring as well as increased electrostatic repulsion between the methanide electron pair and the nitrogen atoms, which can be partly released by formation of Ae–C bonds.

EXPERIMENTAL SECTION

General Remarks. All manipulations were carried out under anaerobic conditions in a nitrogen atmosphere using standard Schlenk techniques. The solvents were dried according to common procedures and were distilled in a nitrogen atmosphere; deuterated solvents were dried over sodium, degassed, and handled under strict exclusion of air and moisture. The yields given are not optimized. Elemental analyses were carried out on a Vario EL III (Elementar) elemental analyzer. ^1H and $^{13}\text{C}\{^1\text{H}\}$ NMR spectra were recorded at 298 K on Bruker AC 200, AC 400, and AC 600 spectrometers. Chemical shifts are reported in parts per million. The bis(trimethylsilyl)amides of magnesium, calcium, strontium, and barium were prepared according to published protocols.²⁹ The preparation of $\text{HC}(\text{Pz}^{\text{Me}_3})_3$ (**1a**) was carried out according to Reger et al.,²⁰ and the synthesis of HPz^{Th} (**4a**) was carried out according to Longhi et al.³⁰

$[\text{Mg}\{\kappa^3\text{N-C}(\text{Pz}^{\text{Me}_3})_3\}_2]$ (**1b**). $\text{HC}(\text{Pz}^{\text{Me}_3})_3$ (0.240 g, 0.71 mmol) was dissolved in 10 mL of THF. After the mixture had cooled to -78°C , 0.35 mL of a 1 M solution of dibutylmagnesium in heptane (0.36 mL, 0.36 mmol) was added dropwise. The reaction mixture was warmed to room temperature, at which point a red solution formed that was stirred for an additional 2 h. Afterward, all volatiles were removed in vacuo. The brown-reddish residue was extracted with toluene, and 264.6 mg of **1b** (0.19 mmol, 53%) crystallized at 4°C within a few days. Characterization: ^1H NMR (400 MHz, $[\text{D}_8]$ toluene): δ 1.55 (s, 18H, H31), 1.78 (s, 18H, H41), 2.46 (s, 18H, H21). $^{13}\text{C}\{^1\text{H}\}$ NMR (150 MHz, $[\text{D}_8]$ toluene): δ 8.3 (C31), 10.8 (C41), 11.3 (C21), 72.7 (C1), 108.4 (C3), 141.9 (C2), 145.9 (C4). MS (DEI, m/z [%]): 702 ($[\text{M}^+]$, 38), 593 ($[\text{M}^+ - \text{Pz}^{\text{Me}_3}]$, 10), 483 ($[\text{M}^+ - 2\text{Pz}^{\text{Me}_3}]$, 12), 363 ($[\text{M}^+ - (\text{Tpm}^{\text{Me}_3})^-]$, 100). IR (neat, cm^{-1}): 2951 m, 2858 w, 1574 w, 1512 w, 1467 m, 1435 m, 1398 m, 1248 s, 1236 m, 1114 m, 1004 w, 874 s, 822 w, 744 s, 549 s. Elemental analysis calcd for $\text{C}_{38}\text{H}_{54}\text{MgN}_{12}$, 703.22: C 64.90, H 7.74, N 23.90. Found: C 64.01, H 7.43, N 23.05.

$[\text{Ca}\{\kappa^3\text{N-C}(\text{Pz}^{\text{Me}_3})_3\}_2]$ (**1c**). $\text{HC}(\text{Pz}^{\text{Me}_3})_3$ (220 mg, 0.65 mmol) was dissolved in 8 mL of THF. A solution of 164 mg of $[(\text{thf})_2\text{Ca}\{\text{N}(\text{SiMe}_3)_2\}_2]$ (0.325 mmol) in 4 mL of THF was added dropwise. During this addition, the slightly yellow reaction mixture turned deep yellow. The solution was stirred for an additional 3 h. All volatiles were removed in vacuo, and the residue was extracted with toluene. Colorless crystals of $[\text{Ca}\{\kappa^3\text{N-C}(\text{Pz}^{\text{Me}_3})_3\}_2]$ (**1c**, 158.9 mg, 0.22 mmol, 68%) were collected after storage of the mother liquor at -20°C for a few days. Characterization: ^1H NMR (400 MHz, $[\text{D}_8]$ toluene): δ 1.77

(s, 18H, H31), 1.86 (s, 18H, H41), 2.42 (s, 18H, H21). $^{13}\text{C}\{^1\text{H}\}$ NMR (150 MHz, $[\text{D}_8]$ toluene): δ 8.4 (C31), 11.6 (C41), 12.1 (C21), 73.3 (C1), 108.2 (C3), 143.3 (C2), 145.3 (C4). MS (DEI, m/z [%]): 719 ($[\text{M}^+]$, 30), 609 ($[\text{M}^+ - \text{Pz}^{\text{Me}_3}]$, 35), 379 ($[\text{CaC}(\text{Pz}^{\text{Me}_3})_3]^+$, 58), 340 ($[\text{L}^+]$, 4). IR (neat, cm^{-1}): 3033 w, 2917 m, 2860 w, 1574 w, 1479 w, 1436 m, 1390 m, 1246 s, 1233 m, 1146 w, 1099 m, 1037 w, 1002 m, 874 s, 845 w, 805 w, 744 m, 734 s, 698 w, 669 s, 573 w, 543 m. Elemental analysis calcd for $\text{C}_{38}\text{H}_{54}\text{CaN}_{12}$, 718.99: C 63.48, H 7.57, N 23.83. Found: C 62.21, H 7.25, N 22.98.

$[\text{Sr}\{\kappa^3\text{N-C}(\text{Pz}^{\text{Me}_3})_3\}_2]$ (**1d**). $\text{HC}(\text{Pz}^{\text{Me}_3})_3$ (225 mg, 0.66 mmol) was dissolved in 8 mL of THF. A solution of $[(\text{thf})_2\text{Sr}\{\text{N}(\text{SiMe}_3)_2\}_2]$ (183 mg, 0.33 mmol) in 5 mL of THF was added dropwise, at which point the reaction mixture turned dark yellow. The solution was stirred for an additional 3 h. All volatiles were then removed in vacuo, and the residue was extracted with toluene. After storage of these combined toluene solutions at -20°C for several days, 154.4 mg of crystalline $[\text{Sr}\{\kappa^3\text{N-C}(\text{Pz}^{\text{Me}_3})_3\}_2]$ (154.3 mg, 0.20 mmol, 61%) was isolated. Characterization: ^1H NMR (400 MHz, $[\text{D}_8]$ toluene): δ 1.70 (s, 18H, H31), 1.84 (s, 18H, H41), 2.35 (s, 18H, H21). $^{13}\text{C}\{^1\text{H}\}$ NMR could not be obtained because of sparing solubility in common organic solvents. MS (DEI, m/z [%]): 767 ($[\text{M}^+]$, 20), 657 ($[\text{M}^+ - \text{Pz}^{\text{Me}_3}]$, 18), 427 ($[\text{M}^+ - \text{Tpm}^{\text{Me}_3}]$, 12), 340 ($[\text{Tpm}^{\text{Me}_3}]$, 26), 231 ($[\text{Bpm}^{\text{Me}_3}]^+$, 100). IR (neat, cm^{-1}): 2914 m, 2857 w, 1577 m, 1508 m, 1434 m, 1382 s, 1345 w, 1320 w, 1279 s, 1245 m, 1232 w, 1096 m, 999 m, 875 s, 846 w, 802 m, 743 s, 732 m, 693 w, 671 w, 540 s. Elemental analysis calcd for $\text{C}_{38}\text{H}_{54}\text{SrN}_{12}$, 766.54: C 59.54, H 7.10, N 21.93. Found: C 59.23, H 6.98, N 21.45.

$[\text{Ba}\{\kappa^3\text{N-C}(\text{Pz}^{\text{Me}_3})_3\}_2]$ (**1e**). $\text{HC}(\text{Pz}^{\text{Me}_3})_3$ (213 mg, 0.62 mmol) was dissolved in 6 mL of toluene. A solution of $[(\text{dme})_2\text{Ba}\{\text{N}(\text{SiMe}_3)_2\}_2]$ (200 mg, 0.31 mmol) dissolved in 4 mL of toluene was added dropwise at room temperature. The resulting solution turned dark yellow and was stirred for an additional 12 h. Removal of all volatiles under reduced pressure and washing with 10 mL of hexane left a yellowish analytically pure powder of **1e** (147.2 mg, 0.18 mmol, 58%). Recrystallization efforts led to decomposition reactions. Characterization: ^1H NMR (400 MHz, $[\text{D}_8]$ toluene): δ 1.56 (s, 18H, H31), 1.73 (s, 18H, H41), 2.40 (s, 18H, H21). $^{13}\text{C}\{^1\text{H}\}$ NMR (150 MHz, $[\text{D}_8]$ toluene): δ 7.9 (C31), 11.6 (C41), 11.7 (C21), 72.2 (C1), 108.1 (C3), 143.0 (C2), 143.7 (C4). MS (Micro ESI pos, m/z [%]): 817.2 ($[\text{M} + \text{H}]^+$, 100). IR (neat, cm^{-1}): 2918 m, 2860 w, 1588 m, 1475 m, 1434 s, 1377 m, 1321 s, 1277 s, 1201 w, 1112 w, 948 w, 887 m, 870 s, 844 s, 777 m, 734 m, 719 m, 695 w, 671 m, 630 w, 569 m. Elemental analysis calcd for $\text{C}_{38}\text{H}_{54}\text{CaN}_{12}$, 816.24: C 55.92, H 6.67, N 20.59. Found: C 55.23, H 6.45, N 20.12.

$\text{HC}(\text{Pz}^{\text{Tp}})_3$ (**2a**). In a 250 mL one-neck flask, 64.57 mmol of 3-thienylpyrazole (9.698 g) and 3.23 mmol of tetrabutylammonium bromide (1.041 g) were mixed and suspended with 150 mL of distilled water. Afterward, 387.4 mmol of sodium carbonate (41.060 g) was added, and an exothermic reaction took place. After the reaction mixture had cooled to room temperature, 32 mL of chloroform was added. The resulting orange mixture was refluxed for 3 days. A black (organic) phase and a white phase formed. Toluene (500 mL) was added; after removal of solids, a brownish-black solution was obtained. The solution was washed three times each with brine and distilled water. The organic phase was dried over sodium sulfate; afterward, the solvent was removed. A tarry-brown oil remained and was dissolved in 50 mL of toluene. A catalytic amount of trifluoroacetic acid (0.150 mL) was added, and the solution was refluxed for 24 h. Then, the reaction mixture was cooled to room temperature, neutralized with sodium hydrogen carbonate, and washed two times each with distilled water and brine. The organic phase was dried over sodium sulfate. The resulting solution was stripped to dryness to give a brown powder. The product was flushed through a plug of silica with a 1:4 hexane/dichloromethane mixture. The charges containing the desired product were combined and evaporated, yielding tris(thienylpyrazolyl)methane (**2a**) as a white solid (4.28 g, 9.29 mmol, 43.2%). Single crystals suitable for X-ray diffraction studies were obtained from a saturated ethanol solution. Characterization: Mp: 172.6°C . ^1H NMR (400 MHz, CDCl_3): δ 8.37 (s, 1H, H1), 7.64 (d, $J = 2.6$ Hz, 3H, H5), 7.34 (dd, $J = 3.6$ Hz, $J = 1.2$ Hz, 3H, H33), 7.25 (dd, $J = 5.1$ Hz, $J = 1.2$ Hz, 3H, H35), 7.03

(dd, $J = 5.1$ Hz, $J = 3.6$ Hz, 3H, H34), 6.54 (d, $J = 2.6$ Hz, 3H, H4). ^{13}C NMR (101 MHz, CDCl_3): δ 148.8 (C3), 135.5 (C31), 130.8 (C5), 127.4 (C34), 125.4 (C35), 124.8 (C33), 104.7 (C4), 83.4 (C1). MS (Micro ESI, m/z [%]): 483 ($[\text{M}^+\text{Na}]^+$, 100). IR (neat, cm^{-1}): 3132 w, 3116 w, 1559 m, 1499 s, 1466 w, 1428 m, 1389 m, 1376 m, 1336 s, 1307 s, 1238 m, 1219 s, 1187 m, 1085 w, 1064 m, 1050 s, 1024 w, 991 m, 912 m, 848 s, 838 s, 799 s, 749 s, 701 s, 620 w, 599 m, 496 w, 436 m. Elemental analysis, recrystallization in a mixture of *n*-hexane and DCM, calcd for $2\text{a}(\text{DCM})_{0.5}$ ($\text{C}_{22.5}\text{H}_{17}\text{ClN}_6\text{S}_3$), 503.07: C 53.72, H 3.41, N 16.71, S 19.12. Found: C 52.65, H 3.22, N 16.66, S 19.42.

$[(\text{dme})\text{Ca}(\text{Pz}^{\text{Tp}})_2]_2$ (**2c**). $\text{HC}(\text{Pz}^{\text{Tp}})_3$ (0.90 mmol) was dissolved in 12 mL of THF and cooled to -40 °C. To this solution was added a solution of $[(\text{thf})_2\text{Ca}\{\text{N}(\text{SiMe}_3)_2\}_2]$ (0.45 mmol) in 4 mL of THF. The resulting reddish reaction mixture was stirred for an additional 3 h at this temperature. All volatiles were removed at room temperature under reduced pressure, and the residue was dissolved in a mixture of toluene and dme. Within a few days at -20 °C, 217.2 mg of colorless crystals of **2c** (0.20 mmol, 46%) precipitated and was collected. Characterization: ^1H NMR (600 MHz, C_6D_6): δ 2.69 (s, 6H, CH_3 -dme), 2.85 (s, 4H, CH_2 -dme), 6.12 (d, $J = 2.61$ Hz, 2H, H4), 6.19 (d, $J = 2.16$ Hz, 4H, H4), 6.61 (t, $J = 3.85$ Hz, $J = 5.31$ Hz, 4H, H34), 6.69 (m, 6H, H35), 6.76 (m, 2H, H34), 7.15 (m, 2H, H33), 7.16 (d, $J = 2.7$ Hz, 2H, H5), 7.22 (d, $J = 2.4$ Hz, 4H, H33), 8.31 (m, 4H, H5). $^{13}\text{C}\{^1\text{H}\}$ NMR (150 MHz, C_6D_6): δ 58.6 (CH_3 -dme), 71.0 (CH_2 -dme), 83.3 (C1), 103.5 (C4), 104.2 (C4), 124.2 (C34), 124.2 (C35), 125.3 (C34), 124.7 (C33), 130.7 (C5), 124.2 (C33), 134.6 (C5), 135.7 (C31), 149.7 (C3). IR (neat, cm^{-1}): 3104 w, 2986 w, 1561 s, 1500 s, 1466 m, 1427 m, 1389 m, 1368 m, 1336 m, 1312 s, 1277 m, 1239 m, 1217 s, 1191 m, 1085 m, 1050 s, 994 m, 913 m, 843 s, 796 s, 752 s, 693 s. Elemental analysis did not give reliable results because of decomposition during isolation and handling of this compound.

Complex **2c** decomposed during handling and recrystallization, yielding calcium bis(3-thienylpyrazolate) and 1,1,2,2-tetrakis(3-thiophen-2-ylpyrazol-1-yl)ethene. To verify these degradation products, alternative preparative pathways were developed.

Tetrakis(3-thiophen-2-ylpyrazol-1-yl)ethene (**4**). Degradation product **3** was obtained by the reaction of **1a** with $\text{Li}\{\text{N}(\text{SiMe}_3)_2\}$, $(\text{thf})_2\text{Ca}\{\text{N}(\text{SiMe}_3)_2\}_2$, $(\text{dme})_2\text{Sr}\{\text{N}(\text{SiMe}_3)_2\}_2$, and $(\text{dme})_2\text{Ba}\{\text{N}(\text{SiMe}_3)_2\}_2$ in dme or THF at room temperature. The solutions turned black; after hydrolysis and extraction with chloroform, the formation of the ethene species was verified. Characterization: ^1H NMR (400 MHz, CDCl_3): δ 6.58 (d, $J = 2.41$ Hz, 2H, H4), 6.78 (d, $J = 2.63$ Hz, 1H, H4), 6.84 (d, $J = 2.41$ Hz, 1H, H4), 7.00 (dd, $J = 5.17$ Hz, $J = 1.48$ Hz, 4H, H34), 7.23 (d, $J = 4.96$ Hz, 4H, H35), 7.41 (d, $J = 5.03$ Hz, 1H, H5), 7.48 (d, $J = 2.64$ Hz, 4H, H33), 7.54 (d, $J = 3.65$ Hz, 1H, H5), 7.66 (d, $J = 2.64$ Hz, 2H, H5). $^{13}\text{C}\{^1\text{H}\}$ NMR (101 MHz, CDCl_3): δ 105.0 (C4), 107.0 (C4), 125.9 (C35), 127.2 (C34), 127.1 (C5), 132.4 (C33), 134.6 (C5), 132.3 (C5), 147.0 (C3), 148.7 (C3), 147.8 (C=C), 150.8 (C31). MS (DEI, m/z [%]): 620 ($[\text{M}^+]$, 52), 471 ($[\text{M}^+ - \text{Pz}^{\text{Tp}}]$, 24), 311 ($[(\text{C}(\text{Pz}^{\text{Tp}})_2]^+$, 100%), 161 ($[(\text{C}(\text{Pz}^{\text{Tp}})]^+$, 99), 149 ($[(\text{Pz}^{\text{Tp}})^+]$, 89). IR (KBr windows, cm^{-1}): 3102 w, 1561 m, 1506 m, 1464 w, 1433 w, 1370 m, 1328 w, 1275 w, 1253 w, 1217 m, 1087 m, 1066 s, 1051 s, 1022 m, 922 m, 973 m, 938 w, 909 m, 869 w, 846 s, 805 s, 766 s, 752 s, 691 s, 605 m. Elemental analysis calcd for $\text{C}_{30}\text{H}_{20}\text{N}_8\text{S}_4$, 620.79: C 58.04, H 3.25, N 18.05, S 20.66. Found: C 58.95, H 4.13, N 17.21, S 19.70.

$[(\text{HPz}^{\text{Tp}})_2\text{Mg}(\text{Pz}^{\text{Tp}})_2]_2$ (**3b**). HPz^{Tp} (0.86 mmol) was dissolved in 10 mL of THF. After the reaction mixture had cooled to -78 °C, 0.35 mL of a 1 M solution of dibutylmagnesium (0.48 mL, 0.48 mmol) in heptane was added dropwise. The reaction mixture was warmed to room temperature, at which point a yellow solution formed that was stirred for an additional 8 h. Afterward, all volatiles were removed in vacuo. The yellowish residue was extracted with a mixture of hot toluene and DME. Crystals suitable for X-ray structure analysis precipitated (132.7 mg, 0.14 mmol, 30%) and were collected. Characterization: ^1H NMR (400 MHz, $[\text{D}_8]\text{THF}$): δ 6.34 (m, 6H, H4), 6.80 (t, $J = 3.82$ Hz, 6H, H34), 7.11 (d, $J = 3.50$ Hz, 6H, H35), 7.16 (m, 6H, H33), 7.76 (s, 6H, H5). $^{13}\text{C}\{^1\text{H}\}$ NMR (100 MHz, $[\text{D}_8]\text{THF}$): δ 101.4 (C4), 122.8 (C33), 123.48 (C35), 126.7 (C34), 128.79 (C5), 138.1 (C31), 146.4 (C3). IR (neat, cm^{-1}): 3130 m,

3022 m, 2959 m, 2911 m, 2873 m, 2807 w, 1582 w, 1561 m, 1519 m, 1463 m, 1409 s, 1372 m, 1354 w, 1342 w, 1312 m, 1274 m, 1215 w, 1191 m, 1178 m, 1116 m, 1084 m, 1069 w, 1047 s, 1030, 938 s, 910 s, 886 s, 872, 845 s, 832 m, 823 m, 756 s, 693 s, 648 s, 604 m, 492 m. Elemental analysis calcd for $\text{C}_{42}\text{H}_{34}\text{MgN}_{12}\text{S}_6$, 922.12: C 54.62, H 3.71, N 18.20, S 20.82. Found: C 53.99, H 3.74, N 17.99, S 20.43.

$[(\text{tmeda})\text{Ca}(\text{Pz}^{\text{Tp}})_2]_2$ (**3c**). HPz^{Tp} (0.84 mmol) was dissolved in 8 mL of THF and added to a solution of $[(\text{thf})_2\text{Ca}\{\text{N}(\text{SiMe}_3)_2\}_2]$ (0.42 mmol) in THF. The resulting yellow solution was stirred for an additional 12 h at room temperature. All volatiles were removed under reduced pressure, and the residue was dissolved in a mixture of toluene and tmeda. Within a few days at room temperature, 175.3 mg of colorless crystals of **3c** (0.2 mmol, 33%) precipitated and was collected. Characterization: ^1H NMR (600 MHz, C_6D_6): δ 2.27 (s, 12H, CH_3 -tmeda), 2.46 (s, 4H, CH_2 -tmeda), 6.68 (m, 2H, H4), 7.05 (t, $J = 3.90$ Hz, 2H, H34), 7.16 (d, $J = 4.94$ Hz, 2H, H35), 7.34 (m, 2H, H33), 7.76 (d, $J = 1.94$ Hz, H5). $^{13}\text{C}\{^1\text{H}\}$ NMR (150 MHz, C_6D_6): δ 46.3 (CH_3), 58.6 (CH_2), 103.2 (C4), 125.9 (C33), 127.7 (C35), 128.8 (C34), 129.6 (C31), 138.4 (C5), 141.0 (C3). IR (neat, cm^{-1}): 3114 m, 3066 m, 2957 m, 2908 m, 2874 m, 2838 m, 2802 m, 1460 s, 1410 s, 1357 m, 1286 m, 1214 m, 1180 m, 1066 s, 1047 s, 1030 s, 1016 s, 937 s, 927 s, 910 s, 844 m, 827 m, 792 m, 773 m, 691 s, 656 m, 603 m. Elemental analysis calcd for $\text{C}_{40}\text{H}_{32}\text{Ca}_2\text{N}_{12}\text{S}_4$, 909.34: C 52.83, H 5.76, N 18.48, S 14.10. Found: C 51.82, H 5.42, N 17.71, S 13.09.

$[(\text{pmdeta})\text{Sr}(\text{Pz}^{\text{Tp}})_2]_2$ (**3d**). HPz^{Tp} (0.96 mmol) was dissolved in 10 mL of THF and added to a solution of $[(\text{dme})_2\text{Sr}\{\text{N}(\text{SiMe}_3)_2\}_2]$ (0.48 mmol) in THF. The resulting yellow solution was stirred for an additional 12 h at room temperature. Then, all volatiles were removed under reduced pressure, and the residue was dissolved in a mixture of toluene and pmdeta. Crystals suitable for X-ray diffraction experiments precipitated and were collected (171.8 mg, 0.30 mmol, 64%). Characterization: ^1H NMR (600 MHz, $[\text{D}_8]\text{THF}$): δ 2.15 (s, 3H, CH_3 -pmdeta), 2.19 (s, 12H, CH_3 -pmdeta), 2.37 (t, $J = 6.24$ Hz, 4H, CH_2 -pmdeta), 2.48 (t, $J = 6.30$ Hz, 4H, CH_2 -pmdeta), 6.40 (s, 2H, H4), 6.91 (dd, $J = 5.46$ Hz, $J = 3.69$ Hz, 2H, H34), 7.04 (d, $J = 4.83$ Hz, 2H, H35), 7.14 (d, $J = 2.94$ Hz, 2H, H33). $^{13}\text{C}\{^1\text{H}\}$ NMR (150 MHz, $[\text{D}_8]\text{THF}$): δ 42.5 (CH_3), 45.9 (CH_2), 57.1 (CH_2), 58.3 (CH_2), 102.1 (C4), 120.6 (C33), 121.3 (C35), 127.0 (C34), 136.0 (C5), 141.3 (C31), 144.5 (C3). IR (neat, cm^{-1}): 3082 m, 2957 m, 2868 m, 2834 m, 2793 m, 1688 w, 1463 s, 1453 s, 1412 s, 1357 m, 1302 m, 1286 m, 1250 m, 1221 m, 1181 m, 1151 m, 1106 m, 1062 m, 1034 s, 1021 s, 980 m, 941 m, 928 s, 912 s, 892 s, 841 s, 828 s, 787 m, 762 m, 750 s, 706 s, 692 s, 642 m, 591 w, 574 w, 500 w, 462 w, 419 s. Elemental analysis calcd for $\text{C}_{23}\text{H}_{33}\text{N}_7\text{S}_2\text{Sr}$, 559.31: C 49.39, H 5.95, N 17.53, S 11.47. Found: C 49.01, H 6.02, N 17.24, S 10.67.

$[(\text{hmteta})\text{Ba}(\text{Pz}^{\text{Tp}})_2]_2$ (**3e**). HPz^{Tp} (0.92 mmol) was dissolved in 10 mL of THF and added to a solution of $[(\text{dme})_2\text{Ba}\{\text{N}(\text{SiMe}_3)_2\}_2]$ (0.46 mmol) in THF. The resulting yellow solution was stirred for an additional 12 h at room temperature. Then all volatiles were removed under reduced pressure, and the residue was extracted with a mixture of toluene and hmteta. Crystals suitable for X-ray diffraction experiments (198.2 mg, 0.29 mmol, 62%) precipitated and were collected. Characterization: ^1H NMR (400 MHz, $[\text{D}_8]\text{THF}$): δ 2.12 (s, 6H, CH_3 -hmteta), 2.19 (s, 12H, CH_3 -hmteta), 2.42 (m, 4H, CH_2 -hmteta), 2.52 (m, 8H, CH_2 -hmteta), 6.41 (d, $J = 1.54$ Hz, 2H, H4), 6.91 (dd, $J = 3.52$ Hz, $J = 1.49$ Hz, 2H, H34), 7.00 (dd, $J = 1.06$ Hz, $J = 5.05$ Hz, 2H, H35), 7.08 (dd, $J = 3.54$ Hz, $J = 1.04$ Hz, 2H, H33), 7.40 (d, $J = 5.46$ Hz, 2H, H5). $^{13}\text{C}\{^1\text{H}\}$ NMR (100 MHz, $[\text{D}_8]\text{THF}$): δ 41.3 (CH_3), 44.9 (CH_2), 56.4 (CH_2), 56.8 (CH_2), 57.2 (CH_2), 102.0 (C4), 119.8 (C33), 120.3 (C35), 126.0 (C34), 135.3 (C5), 141.4 (C31), 143.74 (C3). IR (neat, cm^{-1}): 3100 m, 3069 m, 2957 m, 2828 m, 2785 m, 1542 w, 1456 s, 1411 m, 1357 w, 1310 m, 1291 m, 1261 m, 1216 w, 1176 m, 1159 w, 1134 m, 1098 m, 1060 m, 1031 s, 1021 s, 984 m, 928 m, 910 m, 900 m, 838 s, 828 s, 774 m, 748 s, 703 w, 681 m, 657 s, 642 m, 593 m, 571 w, 410 s. Elemental analysis calcd for $\text{C}_{28}\text{H}_{45}\text{N}_9\text{S}_2\text{Ba}$, 709.17: C 47.42, H 6.89, N 17.78, S 9.04. Found: C 47.92, H 7.40, N 18.17, S 6.33.

X-ray Crystal Structure Determinations. The intensity data for the compounds were collected on a Nonius KappaCCD diffractometer, using graphite-monochromated Mo $K\alpha$ radiation. Data were corrected

for Lorentz and polarization effects; absorption was taken into account on a semiempirical basis using multiple scans.^{31–33}

The structures were solved by direct methods (SHELXS³⁴) and refined by full-matrix least-squares techniques against F_o^2 (SHELXL-97³⁴). The hydrogen atoms bound to compounds **2a**, **3b**, and **3c** without the disordered thp and tmeda ligands were located by difference Fourier synthesis and refined isotropically. All other hydrogen atoms were included at calculated positions with fixed thermal parameters. All nondisordered, non-hydrogen atoms were refined anisotropically.³⁴ The crystal of **3d** was a nonmerohedral twin. The twin law was determined by PLATON³⁴ to $(-1.0\ 0.0\ 0.0)\ (0.0\ -1.0\ 0.0)\ (0.693\ 0.0\ 1.0)$. The contribution of the main component was refined to 0.876(2). The crystal of **1b** contains large voids, which are filled with disordered solvent molecules. The size of the voids is 370 Å³/unit cell. Their contribution to the structure factors was secured by back-Fourier transformation using the SQUEEZE routine of the program PLATON,³⁵ resulting in 54 electrons/unit cell.

The crystals of **4** were extremely thin and of low quality, resulting in a substandard data set; however, the structure is sufficient to show connectivity and geometry despite the high final value of R. We only included the conformation of the molecule and the crystallographic data. We did not deposit the data in the Cambridge Crystallographic Data Centre.

Crystallographic data as well as structure solution and refinement details are listed in the Supporting Information. The software programs XP and POV-Ray were used for the structure representations.^{36,37}

■ ASSOCIATED CONTENT

■ Supporting Information

Molecular structures and numbering schemes of compounds **1b,c**; crystal data and refinement details for **1a–d**, **2a,c**, **3**, **4b–e**; NMR spectra of the reported compounds; energies of the optimized structures for the investigation of the decomposition of tris(amino)methanide [(H₂N)₃C[−]] and tris(pyrazolyl)methanide [(Pz)₃C[−]]; quantum chemical investigation data of [Ca{κ¹C,κ²N-C(Pz^{TP})₃}₂]; optimized structures, geometries, and energies for **A–E**; and CIF files for **1a–d**, **2a,c**, and **3b–e**. This material is available free of charge via the Internet at <http://pubs.acs.org>. Crystallographic data (excluding structure factors) have also been deposited with the Cambridge Crystallographic Data Centre (CCDC) as the following supplementary publications: CCDC-1024356 for **1a**, CCDC-1024357 for **1b**, CCDC-1024358 for **1c**, CCDC-1024359 for **1d**, CCDC-1024360 for **2a**, CCDC-1024361 for **2c**, CCDC-1024362 for **3b**, CCDC-1024363 for **3c**, CCDC-1024364 for **3d**, and CCDC-1024365 for **3e**. Copies of these can be obtained free of charge by application to the CCDC via mail at 12 Union Road, Cambridge CB2 1EZ, U.K. or e-mail at deposit@ccdc.cam.ac.uk.

■ AUTHOR INFORMATION

Corresponding Author

*Fax: +49 3641 948132. E-mail: m.we@uni-jena.de. Homepage: <http://www.lsacl.uni-jena.de/>.

Notes

The authors declare no competing financial interest.

■ ACKNOWLEDGMENTS

We appreciate the financial support of the Verband der Chemischen Industrie (VCI/FCI, Frankfurt/Main, Germany). Infrastructure of the Institute of Inorganic and Analytical Chemistry was partly provided by the EU (European Regional Development Fund, EFRE) and the Friedrich Schiller University Jena. We also thank Patrick Hoffmann for support in the frame of his master studies.

■ REFERENCES

- (1) Trofimenko, S. *Polyhedron* **2004**, *23*, 197–203.
- (2) Yap, G. P. A. *Acta Crystallogr.* **2013**, *C69*, 937–938.
- (3) (a) Trofimenko, S. *Acc. Chem. Res.* **1971**, *4*, 17–22. (b) Trofimenko, S. *Chem. Rev.* **1993**, *93*, 943–980. (c) Trofimenko, S. *Scorpionates: The Coordination Chemistry of Polypyrazolylborate Ligands*; Imperial College Press: London, 1999.
- (4) (a) Santos, I.; Marques, N. *New J. Chem.* **1995**, *19*, 551–571. (b) Kitajima, N.; Tolman, W. B. *Prog. Inorg. Chem.* **1995**, *43*, 419–531. (c) Edelmann, F. T. *Angew. Chem., Int. Ed.* **2001**, *40*, 1656–1660. (d) Marques, N.; Sella, A.; Takats, J. *Chem. Rev.* **2002**, *102*, 2137–2159. (e) Akita, M. *J. Organomet. Chem.* **2004**, *689*, 4540–4551. (f) Paulo, A.; Correia, J. D. G.; Campello, M. P. C.; Santos, I. *Polyhedron* **2004**, *23*, 331–360. (g) Pettinari, C. *Scorpionates II: Chelating Borate Ligands*; Imperial College Press: London, 2008. (h) Spicer, M. D.; Reglinski, J. *Eur. J. Inorg. Chem.* **2009**, 1553–1574. (5) Smith, J. M. *Comments Inorg. Chem.* **2008**, *29*, 189–233. (6) (a) Reger, D. L. *Comments Inorg. Chem.* **1999**, *21*, 1–28. (b) Bigmore, H. R.; Lawrence, S. C.; Mountford, P.; Tredget, C. S. *Dalton Trans.* **2005**, 635–651. (c) Pettinari, C.; Pettinari, R. *Coord. Chem. Rev.* **2005**, *249*, 525–543. (7) (a) Otero, A.; Fernández-Baeza, J.; Antiñolo, A.; Tejada, J.; Lara-Sánchez, A. *Dalton Trans.* **2004**, 1499–1510. (b) Pettinari, C.; Pettinari, R. *Coord. Chem. Rev.* **2005**, *249*, 663–691. (c) Otero, A.; Fernández-Baeza, J.; Lara-Sánchez, A.; Sánchez-Barba, L. F. *Coord. Chem. Rev.* **2013**, *257*, 1806–1868. (8) (a) Kuzu, I.; Kruppenacher, I.; Meyer, J.; Armbruster, F.; Breher, F. *Dalton Trans.* **2008**, 5836–5865. (b) Murkherjee, R. *Coord. Chem. Rev.* **2000**, *203*, 151–218. (c) Klingele, J.; Dechert, S.; Meyer, F. *Coord. Chem. Rev.* **2009**, *253*, 2698–2741. (d) Zhang, J.-P.; Zhang, Y.-B.; Lin, J.-B.; Chen, X.-M. *Chem. Rev.* **2012**, *112*, 1001–1033. (e) García-Antón, J.; Bifill, R.; Escriche, L.; Llobet, A.; Sala, X. *Eur. J. Inorg. Chem.* **2012**, 4775–4789. (9) Han, R.; Parkin, G. *Inorg. Chem.* **1993**, *32*, 4968–4970. (10) Han, R.; Parkin, G. *Inorg. Chem.* **1992**, *31*, 983–988. (11) Naglav, D.; Bläser, D.; Wölper, C.; Schulz, S. *Inorg. Chem.* **2014**, *53*, 1241–1249. (12) Sohrin, Y.; Matsui, M.; Hata, Y.; Hasegawa, H.; Kokusen, H. *Inorg. Chem.* **1994**, *33*, 4376–4383. (13) Reger, D. L.; Little, C. A.; Smith, M. D.; Rheingold, A. L.; Liable-Sands, L. M.; Yap, G. P. A.; Guzei, I. A. *Inorg. Chem.* **2002**, *41*, 19–27. (14) Cushion, M. G.; Meyer, J.; Heath, A.; Schwarz, A. D.; Fernández, I.; Breher, F.; Mountford, P. *Organometallics* **2010**, *29*, 1174–1190. (15) Meyer, J.; Kuzu, I.; González-Gallardo, S.; Breher, F. *Z. Anorg. Allg. Chem.* **2013**, *639*, 301–307. (16) Kratzert, D.; Leusser, D.; Stern, D.; Meyer, J.; Breher, F.; Stalke, D. *Chem. Commun.* **2011**, *47*, 2931–2933. (17) Bigmore, H. R.; Meyer, J.; Kruppenacher, I.; Rügger, H.; Clot, E.; Mountford, P.; Breher, F. *Chem.—Eur. J.* **2008**, *14*, S918–S934. (18) Müller, C.; Görls, H.; Kriek, S.; Westerhausen, M. *Eur. J. Inorg. Chem.* **2013**, 5679–5682. (19) Cushion, M. G.; Mountford, P. *Chem. Commun.* **2011**, *47*, 2276–2278. (20) Reger, D. L.; Elgin, J. D.; Smith, M. D.; Grandjean, F.; Rebbouh, L.; Long, G. J. *Eur. J. Inorg. Chem.* **2004**, 3345–3352. (21) (a) Westerhausen, M. *Coord. Chem. Rev.* **1998**, *176*, 157–210. (b) Westerhausen, M. *Trends Organomet. Chem.* **1997**, *2*, 89–105. (22) (a) Halcrow, M. A. *Dalton Trans.* **2009**, 2059–2073. (b) Torvisco, A.; O'Brien, A. Y.; Ruhlandt-Senge, K. *Coord. Chem. Rev.* **2011**, *255*, 1268–1292. (23) (a) Hanusa, T. P. *Coord. Chem. Rev.* **2000**, *210*, 329–367. (b) Alexander, J. S.; Ruhlandt-Senge, K. *Eur. J. Inorg. Chem.* **2002**, 2761–2774. (24) Westerhausen, M.; Langer, J.; Kriek, S.; Fischer, R.; Görls, H.; Köhler, M. *Top. Organomet. Chem.* **2013**, *45*, 29–72. (25) Kassae, M. Z.; Ghambarian, M.; Musavi, S. M.; Shakib, F. A.; Momeni, M. R. *J. Phys. Org. Chem.* **2009**, *22*, 919–924.

- (26) Gronert, S.; Keeffe, J. R.; O'Ferrall, R. A. M. *J. Am. Chem. Soc.* **2011**, *133*, 3381–3389. Corrigendum: Gronert, S.; Keeffe, J. R.; O'Ferrall, R. A. M. *J. Am. Chem. Soc.* **2011**, *133*, 11817–11818.
- (27) (a) Arduengo, A. J.; Davidson, F.; Krafczyk, R.; Marshall, W. J.; Tamm, M. *Organometallics* **1998**, *17*, 3375–3382. (b) Schumann, H.; Gottfriedsen, J.; Glanz, M.; Dechert, S.; Demtschuk, J. *J. Organomet. Chem.* **2001**, *617–618*, 588–600. (c) Herrmann, W. A.; Köcher, C. *Angew. Chem., Int. Ed. Engl.* **1997**, *36*, 2162–2187.
- (28) Cosgriff, J. E.; Deacon, G. B. *Angew. Chem., Int. Ed.* **1998**, *37*, 286–287.
- (29) Westerhausen, M. *Inorg. Chem.* **1991**, *30*, 96–101.
- (30) Longhi, K.; Moreira, D. N.; Marzari, M. R. B.; Floss, V. M.; Bonaccorso, H. G.; Zanatta, N.; Martins, M. A. P. *Tetrahedron Lett.* **2010**, *51*, 3193–3196.
- (31) Hooft, R. *COLLECT Data Collection Software*; Nonius B.V.: Almere, The Netherlands, 1998.
- (32) Otwinowski, Z.; Minor, W. Processing of X-ray Diffraction Data Collected in Oscillation Mode. In *Macromolecular Crystallography, Part A*; Carter, C. W., Sweet, R. M., Eds.; Methods in Enzymology Series, Vol. 276; Academic Press: New York, 1997; pp 307–326.
- (33) SADABS, version 2.10; Bruker-AXS: Madison, WI, 2002.
- (34) Sheldrick, G. M. *Acta Crystallogr.* **2008**, *A64*, 112–122.
- (35) Spek, A. L. *Acta Crystallogr.* **2009**, *D65*, 148–155.
- (36) XP; Siemens Analytical X-ray Instruments: Madison, WI, 1994.
- (37) POV-Ray; Persistence of Vision Raytracer: Victoria, Australia, 2007.